UDC 629.735.015.4:620.179.1(042.3)

FEATURE OF D16AT ALUMINUM ALLOY DEFORMATION RELIEF EVOLUTION UNDER VARIABLE AMPLITUDE LOADING

S. Yutskevych, PhD

National Aviation University

s.yutskevych@bigmir.net

Describes feature of deformation relief formation on the D16AT duralumin alloy alclad surface under variable amplitude loading. Quantitative deformation relief parameters can be used for aircraft skin boundary state prediction methods developing.

Keyword: fatigue, deformation relief, variable amplitude loading, boundary state.

Описано особливості процесу формування деформаційного рельєфу на поверхні плакованого шару дюралюмінієвого сплаву Д16АТ при випадковому навантажуванні. Кількісні параметри, які описують деформаційний рельєф, характеризують пошкоджуваність матеріалу і можуть бути використані для розробки методів прогнозування граничного стану обшивки літака.

Ключові слова: втома, деформаційний рельєф, випадкове навантажування, граничний стан.

Introduction

One of the most major problems for aviation structure is the problem of physical and mechanical properties of materials changes assessment during aircraft operation. First of all, it is connected with necessity of aircraft residual life estimation experimental and theoretical methods accuracy increasing. Key element for this task solution is information about aircraft structure element current state.

Analysis of researches and publications

Nowadays leading aviation design bureau are engaged in aircraft Structure Health Monitoring (SHM) system development, that allows to obtain necessary information about structure state [1]. So, for example, the Airbus Company suggested basic approach according to which non-destructive testing technology will became an integral part of the aircraft structure. In this case different techniques can be used such as measuring loads and predicting actual fatigue life or sending waves being either of an acoustic, electromagnetic, thermal or any other physical nature through the structure for direct damage monitoring. Different implementations of these methods as well as sensors are available or are under development [2].

Among different SHM sensors special place takes the Deformation Relief (DR) fatigue sensor, developed in NAU and representing compact specimen of D16AT alclad aluminum alloy which fasten to controlled object [3]. Under cyclic loading there is the intensive plastic deformation of alclad, leading to DR formation on the sensor surface which acts as the indicator of the cumulated damage. However, broad application alloy D16AT as a material for aircraft skin allows to obtain information of material current state by DR which is formed in places of stress concentration.

One way of the DR evolution investigation is applying of noncontact interfere profilers [4], that allows to study feature of DR behavior of alclad alloys under fatigue.

Problem statement

The idea of DR evolution investigation under variable amplitude loading is connected with problem of boundary state of D16AT material prediction.

Task solution

Variable amplitude loading fatigue tests were conducted on flat specimen from structural sheet aluminum alloy D16AT on BiSS Bi00-202V digitally controlled servohydraulic test machine. Loading carries out according MiniTWIST standardized load sequences [5]. Originally, the specimen surface is alclad with technically pure aluminum, wherein the cladding layer has 50 μm thickness. In centre the specimen has 4 mm diameter hole, modeling rivet hole in aircraft skin. Specimen surface zone, adjoining to the hole, was polished by diamond paste.

Periodically the fatigue test interrupts for specimen surface condition monitoring. DR changes were controlled on the surface zone with $225 \times 170\ \mu m^2$ dimension, located near hole in the stress concentrator effective range. Every specimen has 4 control zones, two from both sides of the hole. The specimen alclad surface control zones were inspected with interfere optical nano-profiler Micron Alpha [6]. This device allows to register optical image of the surface with DR marks, carries out digital image processing and determines 3D topography of inspected zone. During surface monitoring were defined next parameters: deformation relief saturation; surface roughness and surface plastic deformation.

During cyclic loading with use of the optical microscope which is a part of the profiler, specimen control zone was digitally photographed (fig. 1, *a*). DR in photos is shown as dark spots.

Digital photos of control surface were transformed into the black-and-white image (fig. 1, *b*) by means of which in an automatic mode the total area of DR (S) were estimated. DR saturation quantitative assessment is given by the following function:

$$D = \frac{S}{A}, \quad (1)$$

where *A* is an investigated zone area.

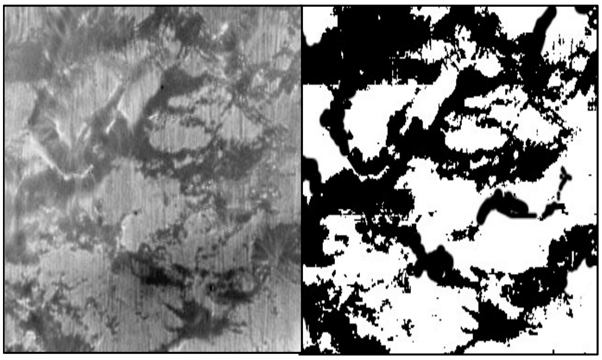

a *b*

Fig. 1. Control surface photo (*a*) and its black-and-white interpretation (*b*)

DR formation in normal to a surface direction was characterised by roughness parameter change which is equal to average value of a real surface deviations from average line (fig. 2):

$$R_a = \frac{1}{n}\sum_{i=1}^{n}|z_i|, \quad (2)$$

where *n* is a number of measurement points.

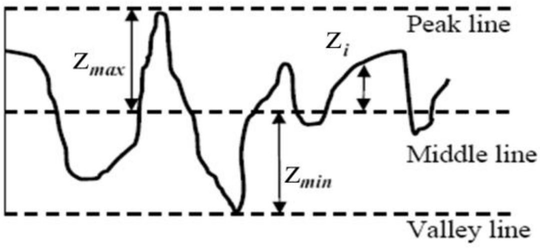

Fig. 2. R_a estimation along the line

The control zone was quantized into 320 lines with 170 microns length and according to the equitation (2) were calculated R_{ai} for them. Value of roughness parameter for control zone was defined as average value for all lines R_{ai}.

Control zone roughness evolution under cyclic loading was characterised by R_a increment parameter:

$$\Delta R_a = R_{ai} - R_{a0}, \quad (3)$$

where R_{a0} roughness parameter value before cyclic loading (an initial roughness), and R_{ai} is after operating time.

Relief change leads to the surface area increasing (fig. 3):

$$\Delta A = A_i - A_0, \quad (4)$$

where A_0 is surface area before cyclic loading; A_i is the surface area after operating time cycles.

For the control zone surface area calculation the x, y plane projection of control zone was represented in the form of a grid with 320×240 integer grid points and the values of surface relief height z_i (measured by means of profiler) correspond to this points (fig. 3). The surface was defined by rectangular grid with z_i in integer grid points. The total area is a sum of triangles areas.

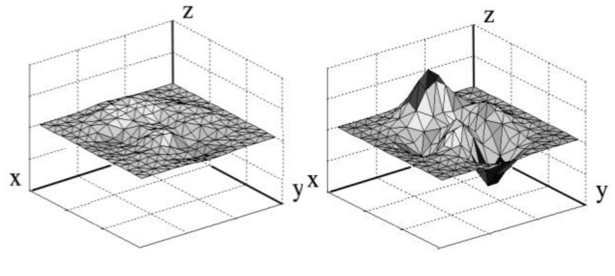

a *b*

Fig. 3. Scheme for initial A_0 (*a*) and after operating time cycles A_i (*b*) surface area estimation

Plastic deformation was defined by surface area change:

$$\varepsilon_a = \frac{\Delta A}{A_0}. \quad (5)$$

Local plastic deformation formation and propagation on cladding layer surface take place from first cycles.

For different three mean stress levels of load sequences results comparison (80 MPa, 90 MPa, 100 MPa), *D* versus *N* relations were shown in relative number of flights $\overline{N} = N_i / N_c$, where N_i — current number of cycles, and N_c — number of cycles before 0,5 mm length crack initiation from control zone side. It is estimated that *DR* saturation development practically does not depend on stress level of load cycle (fig. 4) and can be described as a power function:

$$D = 0{,}388\ \overline{N}^{\,0{,}48}. \quad (6)$$

Relation (6) shows that *DR* saturation is the generalised lifetime characteristic before crack in D16AT alloy initiation. According to the formula (6) irrespective of applied stress levels a crack will initiate at constant *DR* saturation boundary value $D^* \cong 0{,}388$ (at $\overline{N} \to 1$).

This fact testifies about fundamental meaning of DR saturation characteristic and gives the possibility to use parameter D for problem-solving of D16AT alloy lifetime under fatigue prediction.

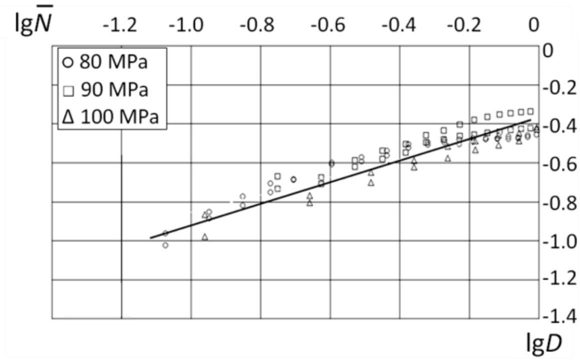

Fig. 4. *DR* saturation change due to relative number of cycles spent in the 0,5 mm crack formation for different stresses levels σ_m

DR is formed not only in specimen surface plane, but also in normal to the specimen surface direction during cyclic loading. The roughness parameter increases with number of flights. Unlike DR saturation surface roughness change depends on applied stress level σ_m. For relative increment $\Delta\overline{R}_a = \Delta R_a / R_{a0}$ versus relative number of flights $\overline{N}$ relations in double logarithmic charts straight lines with approximately identical angle of inclination could be fitted (fig. 5).

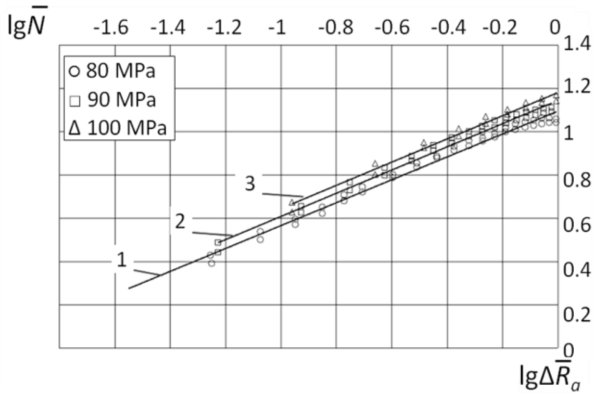

Fig. 5. Roughness increment change due to relative number of cycles spent in the 0,5 mm crack formation for different applied stress levels: σ_m: 1 — 80 MPa; 2 — 90 MPa; 3 — 100 MPa

The results are generalized on fig. 6:

$$\Delta\overline{R}_a = 1{,}93\cdot10^{-4}\sigma_m \;\; \sigma_m + 703{,}6 \;\; \overline{N}^{0{,}53}, \qquad (7)$$

where σ_m is in MPa.

From empirical formulas (6) and (7) the function describing *DR* development on alclad surface during cyclic loading in 3*D*: on planes (parameter *D*) and in a normal to surfaces direction (parameter $\Delta\overline{R}_a$), follows:

$$\Delta\overline{R}_a = 0{,}548\cdot10^{-3}\sigma_m \;\; \sigma_m + 703{,}6 \;\; D^{1{,}1}, \qquad (8)$$

where 80 MPa $\le \sigma_m \le$ 100 MPa.

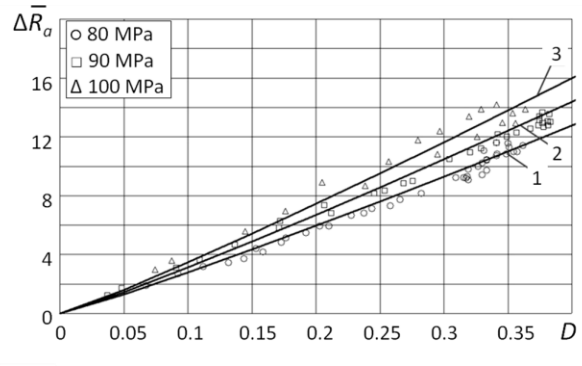

Fig. 6. Roughness increment change due to relative number of cycles spent in the 0,5 mm crack formation for different applied stress levels: σ_m: 1 — 80 MPa; 2 — 90 MPa; 3 — 100 MPa

DR development experimental data at various stress levels of load σ_m argue about equation (8) adequacy (fig. 7).

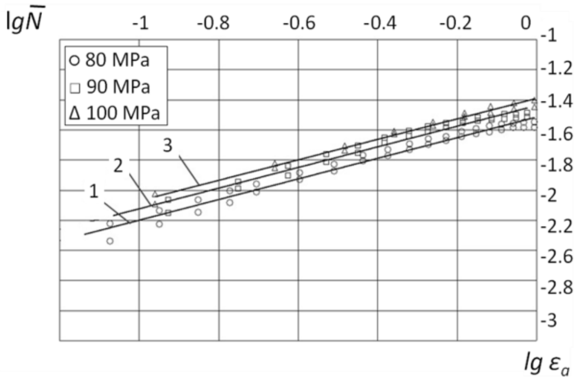

Fig. 7. Plastic deformation changes due to relative number of cycles spent in the 0.5 mm crack formation for different applied stress levels: σ_m: 1 — 80 MPa; 2 — 90 MPa; 3 — 100 MPa

During cyclic loading area of alclad layer surface and irreversible deformation increase (fig. 7).

ε_a versus operating time relatives are approximated by a power function and in a large measure depend on applied stress levels σ_m (fig. 7).

The derived results are described by relation

$$\varepsilon_a = 1{,}09\cdot10^{-6}\sigma_m \;\; \sigma_m + 275{,}3 \;\; \overline{N}^{0{,}68}, \qquad (9)$$

where σ_m is in MPa.

Surface plastic deformation is a result of *DR* development in 3*D*. Having replaced in equation (9) $\overline{N}$ from (6) and σ_m from (8), it will obtain the generalised relation of plastic deformation versus parameters D and $\Delta\overline{R}_a$, characterising DR on the surface

$$\varepsilon_a = 4{,}16 \cdot 10^{-6} \sigma_m \;\; \sigma_m + 275{,}3 \;\; D^{1{,}42}. \qquad (10)$$

As noted above, crack will initiate ($\overline{N} = 1$) when $D^{*} \cong 0{,}388$. Having replaced the given value in the formula (10), it will obtain the ratio between ε_a^* and $\Delta\overline{R}_a^*$, corresponding to a boundary *DR* development condition:

$$\varepsilon_a^* = \left(\sqrt{1 + 0{,}0416 \cdot \Delta\overline{R}_a^*} - 1 \right) \times \left(0{,}13\sqrt{1 + 0{,}0416 \cdot \Delta\overline{R}_a^*} - 0{,}03 \right). \qquad (11)$$

The equation (11) is based on generalisation and approximation of the empirical data having original values scattering. Fig. 8 shows ε_a^* versus $\Delta\overline{R}_a^*$ relation based on the equation (11).

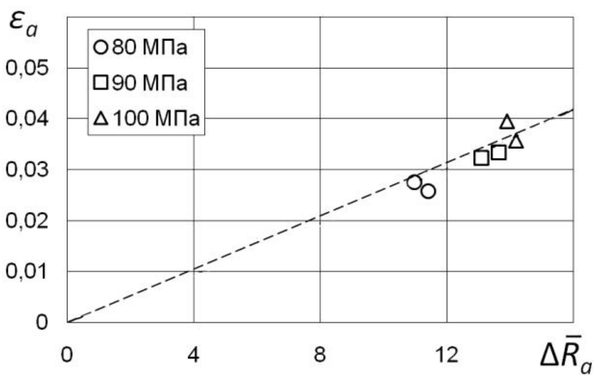

Fig. 11. The surface plastic deformation versus surface roughness relation (before 0,5 mm fatigue crack initiation).

Linear function gives a very good approximation ($R^2 = 0{,}9989$) for equation

$$\varepsilon_a^* \cong 2{,}8 \cdot 10^{-3} \Delta\overline{R}_a^*. \qquad (12)$$

Conclusion

DR evolution on aluminium alloy alclad surface complex research methodology is developed. The given methodology is based on use of contactless interfere profiler Micron-Alpha.

During variable amplitude cyclic loading on D16AT alloy alclad surface *DR* is formed and develops. With number of flights increasing the surface area with *DR* marks and surface roughness increase too. These processes lead to the surface plastic deformation.

The power functions describe the roughness and surface plastic deformation versus number of flights relations and show their dependence from applied stress level. At the moment of crack initiation the boundary values of roughness and plastic deformation are interdependent for any maximum stress levels of loads.

REFERENCES

1. *Bartelds G.* Aircraft structural health monitoring, prospects for smart solutions from a european viewpoint / G. Bartelds // NLR TP 97489. — Amsterdam, 1997. — 13 p.

2. *Structural* health monitoring (SHM) — overview on technologies under development. — Available from Internet: http://www.ndt.net/article/wcndt2004/pdf/aerospace/563_henrich.pdf.

3. *Zasimchuk E. E.* Single-crystals as an indicator of fatigue damage / E. E. Zasimchuk, A. I. Radchenko, M. V. Karuskevich // Fatigue Fract. Engng. Mater. Struct. — 1992. — V. 15, N 12. — P. 1281–1283.

4. *Ignatovich S. R.* Methodical aspects of alloy D16AT deformation relief registration under cyclic loads / S. R. Ignatovich, S .S.Yutskevych, E. Ju. Doroshenko, S. V. Priluckiy // Safety in Aviation and Space Technology: Proceeding of the Fourth World Congress "Aviation in the XXI-st Century"(21-23 September, 2010). — V.1, Kyiv, 2010. — P. 13.17–13.20.

5. *Lowak H.* MiniTWIST. A shortened version of TWIST / H. Lowaк, J. B. De Jonqe, D. Schutz // LBF Bericht FB-106 (NLR 79018U). — Darmstadt-Amsterdam, 1979. — 38 p.

6. Surface quality control with an interference profilometer.

7. Available from Internet: http://old.nau.edu.ua/en/ Science/GotoviRozrobky/MicronAlpha/

Article received 04.03.13.